Han *et al. Applied Biological Chemistry* (2022) 65:37
https://doi.org/10.1186/s13765-022-00704-y

KSABC
The Korean Society for Applied Biological Chemistry

ARTICLE Open Access

Identification of peroxiredoxin II and its related molecules as potential biomarkers of dermal mesenchymal stem cell homing using network analysis

Ying-Hao Han[1*†], Ying-Ying Mao[1†], Yao-Yuan Feng[1], Hong-Yi Xiang[1], Hu-Nan Sun[1], Mei-Hua Jin[1] and Taeho Kwon[2*]

Abstract

In this study, we performed RNA sequencing of Prx II$^{+/+}$ and Prx II$^{-/-}$ dermal mesenchymal stem cells (DMSCs) to identify differentially expressed genes (DEGs). To explore the role of Prx II in DMSCs, we performed Gene Ontology analysis of the DEGs. The results showed that the DEGs were mainly involved in the biological processes of cell migration, intercellular adhesion, and coordination of the regulation of stem cell homing. Through the construction of protein–protein interaction network, four hub genes *Cd274*, *Ccl5*, *Il1b*, and *Stat1* involved in cell adhesion and cell homing were screened. Quantitative reverse transcription PCR analysis showed that *Cd274*, *Ccl5*, *Il1b*, and *Stat1* were down regulated in Prx II$^{-/-}$ DMSCs. miRwalk and Starbase databases were further used to screen the upstream molecules miRNA and lncRNA regulating hub gene. Prx II was found to be involved in the regulation of stem cell homing via the Tctn2/miR-351/Stat1/Il1b axis. Thus, we demonstrated that Prx II is a key molecule in the regulation of the homing ability of DMSCs. Our results provide a theoretical foundation for improving the homing ability of DMSCs by targeting Prx II.

Keywords: Prx II, Dermal mesenchymal stem cell, Differentially expressed gene, Cell migration, Cell–cell adhesion, MicroRNA, Long non-coding RNA

Introduction

Mesenchymal stem cells (MSCs) are considered as a promising stem cell source for regenerative medicine [1]. Their strong differentiation ability and immune regulation activity play key roles in tissue repair. The therapeutic effect of MSCs mainly depends on their specific homing to the injured site. Several studies have shown that when the body experiences ischemia, hypoxia, or other injuries, endogenous or exogenous MSCs with limited efficiency exhibit homing to the inflamed area and injured tissue [2, 3]. After homing to the site of injury, MSCs exert a therapeutic role either by leading to tissue differentiation and injured cell replacement or by secreting various cytokines to promote angiogenesis and regulate the inflammatory response. Although MSCs have an inherent ability to migrate to the injured or inflamed site, owing to the limitations of the signal pathways that regulate cell movement, their homing efficiency is limited [4, 5]. In fact, most injected MSCs cannot reach the site of injury, making it difficult to achieve the expected clinical effect. Therefore,

†Ying-Hao Han and Ying-Ying Mao contributed equally to this work

*Correspondence: hyhbynd@163.com; kwon@kribb.re.kr

[1] College of Life Science and Technology, Heilongjiang Bayi Agricultural University, Daqing, 2 Xinyanglu, Daqing, Heilongjiang 163319, People's Republic of China
[2] Primate Resources Center, Korea Research Institute of Bioscience and Biotechnology (KRIBB), 351-33 Neongme-gil, Ibam-myeon, Jeongeup-si, Jeonbuk 56216, Republic of Korea

identifying methods that can improve the homing rate of MSCs and their clinical efficacy has become an important research focus.

MSCs can be mobilized and enter into the circulation. Alternatively, MSCs can be recruited from the circulation to their original location. Studies have shown that chemokines and their receptors control MSC homing mobilization and migration [6, 7]. The chemokine (C–C motif) ligand 5 (CCL5) can enhance the migration ability of adipose and dermal MSCs (DMSCs) [8]. In an Alzheimer's disease mouse model, researchers detected an increase in CCL5 expression in bone marrow-derived MSCs in the mouse brain [9]. Furthermore, some researchers found that CX3CL1 expression was upregulated in injured brain tissue. CX3CL1 can bind to its receptor, CX3CR1, to induce MSC migration to the brain [10]. In addition, the chemokines CXCL12, CXCL13, CXCL16, CCL11, and CCL2 can promote two-way migration of bone marrow MSCs and human bone marrow endothelial cells [6]. Hence, chemokines and their receptors play important roles in MSC migration and homing.

After MSC mobilization, migration, and homing, MSCs start to adhere to capillary wall endothelial cells. In this process, cell adhesion molecules expressed by MSCs bind with adhesion molecule ligands present in the extracellular matrix. The main adhesion molecules expressed by MSCs and bind to endothelial cells are integrins and selectins. The integrin vascular cell adhesion molecule-1/very late antigen-4 (VLA-4) plays an important role in tight adhesion [11]. The adhesion between endothelial cells and human MSCs treated with VLA-4 antibody was significantly decreased in shear blood flow, suggesting that adhesion of MSCs depends on VLA-4 [12]. Thus, adhesion molecules are indispensable components of the MSC homing process.

Peroxiredoxins (Prx) belong to the peroxidase family of antioxidant proteins, which are widely present in the body. Peroxiredoxin II (Prx II) contains two highly conserved cysteine residues with redox activity, which can rapidly remove low concentrations of active oxygen in vivo [13]. Recent studies have shown that Prx II regulates various stem cells. Silencing of Prx II in colon cancer stem cells led to decreased Nanog expression and cell proliferation [14]. Furthermore, Prx II regulates embryonic stem cell differentiation into neural cells [15]. Studies have demonstrated that the expression of SOX2 and OCT4 was decreased in Prx II-silenced Huh7-H-RasG12V cells [16, 17]. Furthermore, Prx II was found to protect DMSCs from premature senescence [18–20]. These results indicate that PrxII regulates the proliferation, differentiation, and senescence of stem cells, and that it may be a key regulator of stem cell function.

In this study, we used RNA sequencing to analyze the differentially expressed genes (DEGs) between Prx $II^{+/+}$ and Prx $II^{-/-}$ DMSCs derived from mice. Bioinformatics tools were used to perform Gene Ontology (GO) biological process enrichment analysis. The GO term enrichment analysis showed that the DEGs in Prx $II^{-/-}$ DMSCs were mainly related to stem cell migration. Using the STRING database and Cytoscape software, we screened hub genes related to the Prx II-regulated homing of DMSCs, which revealed the homing mechanism of stem cells at the molecular level based on potential key microRNAs (miRNAs) and long non-coding RNAs (lncRNAs) included in the miRWalk and Starbase databases. Our study provides insights into stem cell treatment for various diseases.

Materials and methods

Ethics statement

This study was approved by the Animal Ethics Committee of Heilongjiang Bayi Agricultural University (Approval number: TDJH202116) and was strictly carried out under the guide for the care and use of laboratory animals.

Chemicals

Culture dishes (100 mm) were purchased from NEST Biotechnology (Wuxi, China), fetal bovine serum and penicillin/streptomycin were purchased from Solarbio (Beijing, China), and TRIzol was purchased from Sigma (St. Louis, MO, USA). We used the inNovaUscript II All in One First strand cDNA Synthesis SuperMix kit (Innovagene, Hunan, China), inNova Taq SYBR Green qPCR Mix (Innovagene), miRNA First Strand cDNA Synthesis (Tailing Reaction) (B532451-0010; Sangon Biotech, Shanghai, China), miRNA qPCR Kit (SYBR Green Method) (Sangon Biotech), and a CFX96 real-time PCR system (Bio-Rad, Hercules, CA, USA).

Isolation of DMSCs

DMSCs were isolated and characterized according to standard protocols [21], which our laboratory has also reported on previously [22, 23]. Prx II-rescued cells (referred to as WT) and Prx II gene knockout 129/SVJ mice were maintained in a pathogen-free facility (20–22 °C, humidity 50–60%, and 12-h-dark/light cycle). Briefly, neonatal mice were anesthetized with isoflurane (1.5–2% for induction anesthesia; 1–1.5% for maintenance of anesthesia). We isolated the skin from neonatal 129/SvJ mice and Prx II knockout 129/SvJ mice (aged 1–2 days) for 5 min. After removing the skin, the mice were placed in a euthanasia box that received CO_2 at a rate of 10–30% of the volume of the euthanasia box every minute. The mice were confirmed to be motionless,

non-breathing, and to have dilated pupils for 30 s. After ceasing the CO_2 input, the mice were observed for another minute to confirm their death. The skin samples were digested in 0.25% trypsin-EDTA so that the dermal layer was isolated from the epidermal layer. The dermis was cut into approximately 1 cm^2 pieces and then digested with 0.25% trypsin-EDTA for about 1 h and seeded in DMEM/F12 medium.

Cell culture

The cells were cultured in standard DMEM/F12 medium supplemented with 10% fetal bovine serum and 1% penicillin/streptomycin at 37 °C in a 95% air/5% CO_2 incubator. The culture medium was refreshed every day. When cells reached 90% confluence, they were subcultured after treatment with a 0.25% trypsin-EDTA mixture.

RNA sequencing

mRNA was isolated from total RNA by separating the poly-A containing molecules using poly-T primers. RNA fragmentation, first- and second-strand cDNA syntheses, end repair, adaptor ligation, and PCR amplification were performed. The average size of the cDNA in the sequencing libraries was approximately 160 bp (excluding the adapters). The RNA integrity and quantity of the cDNA libraries were validated before sequencing. The cDNA libraries were clustered onto a TruSeq paired-end flow cell and sequenced using an Illumina HiSeq 2000 Sequencer, producing 100-bp paired-end reads (2×100). RNA sequencing was performed at Gminix.

Functional enrichment analysis

GO analysis is widely used in functional studies and gene set enrichment analysis. The DAVID gene annotation tool [24] was used to analyze GO term enrichment among the DEGs. Targeting graphs of salient functions in three categories, i.e., biological process, molecular function, and cellular component, were constructed to understand the biological functions of the DEGs. We selected $P < 0.05$ and $FC > 1.2$ or < 0.83333 to indicate that genes with a difference of > 1.2 times were DEGs. The biological process terms were analyzed using ClueGo in Cytoscape v3.8.2 to visualize DEG enrichment [25].

Intercellular adhesion and cell migration in GO, construction of a protein–protein interaction (PPI) network, and identification of hub genes

The STRING 10 database provides known and predicted protein interactions based on confidence. These interactions include direct (physical) and indirect (functional) associations originating from the genomic background, experiments, co-expression, and previous knowledge [26]. Genes involved in regulating cell migration and the cell adhesion module were considered as seed nodes and mapped to the STRING database to construct an extended PPI network with a medium confidence score of 0.4. All PPI networks were visualized using Cytoscape v3.8.2 software and a network analyzer tool to calculate the parameters of intermediate betweenness centrality (BC) and degree. Betweenness centrality reflects the number of shortest paths through a node, which is very important in node importance analysis. The degree indicates the number of specific protein interactions. In the final network, the height node is displayed in a large circle, whereas green and blue shadows indicate the BC value of the node from high to low. In this study, nodes with a BC threshold > 0.05 and a degree greater than the average were considered hub genes.

Prediction of pivotal miRNAs and construction of an mRNA–miRNA interaction network

The hub genes in key pathways were selected, and their targeted miRNAs were predicted using miRWalk v2.0 [27]. To verify the accuracy of the results, five databases were used, including TargetScan, miRanda, miRDB, miRWalk, and RNA22. To obtain the target miRNAs of hub genes, an mRNA–miRNA visualization network was constructed using Cytoscape v3.8.2, and target miRNAs for more than two hub genes were selected for further analysis.

miRNA–lncRNA prediction

The Starbase v2.0 tool was used to predict lncRNAs upstream of the selected miRNAs to identify lncRNAs regulating these miRNAs [28]. An lncRNAs–miRNA visual network was constructed using Cytoscape. Finally, the intersection of each miRNA prediction result was obtained.

Table 1 Primer sequences

ID	Sequence(5′-3′)
Cd274 F	CTGGACCTGCTTGCGTTAGTGG
Cd274 R	CCCCTGAAGTTGCTGTGCTGAG
Il1bF	CACTACAGGCTCCGAGATGAACAAC
Il1b R	TGTCGTTGCTTGGTTCTCCTTGTAC
Stat1 F	TCACAGTGGTTCGAGCTTCAG
Stat1 R	CGAGACATCATAGGCAGCGTG
Ccl5 F	GACACCACTCCCTGCTGCTTTG
Ccl5 R	CTCTGGGTTGGCACACACTTGG
mmu-miR-466l F	CGGCCGTATAAATACATGCACACAT
mmu-miR-484 F	TATCAGGCTCAGTCCCCTCC
mmu-miR-351F	TCCCTGAGGAGCCCTTTGAG
lncRNA Tctn2 F	CGCCGTTCCTTGGTCACTTCTAC
lncRNA Tctn2 R	CGTGGTCATAATGGGATCTCCTTGC

Lentivirus-mediated rescue of Prx II

To construct lentiviral vectors to rescue Prx II expression in Prx II$^{-/-}$ DMSCs, the murine full-length Prx II cDNA was used as a PCR template to clone Prx II into the LV5 plasmid, and an empty vector was used as the control. Vectors were purchased from Suzhou GenePharma (Suzhou, China). DMSCs were seeded into 6-well plates at 3×10^5 cells/well and grown to 70–80%. Viral stock at a multiplicity of infection of 60 and 10 mg/mL polybrene were added to the DMSCs. WT cells and control cells (referred to as NC) were harvested.

Verification of hub gene, miRNA, and lncRNA expression using quantitative reverse transcription (RT-q) PCR

Total RNA was extracted from DMSCs using TRIzol reagent. RNA was quantified using a Nanodrop 2000 system (Wilmington, DE, USA) and reverse-transcribed using a cDNA synthesis kit. qPCRs were run using SYBR Green Master Mix on a CFX96 real-time PCR system. Oligonucleotide primers were synthesized and designed at Sangon Biotech and are listed in Table 1. The relative expression levels of hub genes, miRNAs, and lncRNAs were calculated using the $2^{-\Delta\Delta Cq}$ method.

Statistical analysis

Results are expressed as mean ± standard deviation (SD) of three independent experiments and were analyzed by GraphPad Prism 6.0 (GraphPad Software Inc., La Jolla, CA, USA). Student's unpaired t-tests were performed. A P-value less than 0.05 was considered significant. IBM SPSS Statistics Version 25 was used for statistical analysis.

Results

Functional enrichment analysis

In our previous study, we used RNA sequencing to analyze and compare somatic Prx II$^{+/+}$ and Prx II$^{-/-}$ DMSCs. The results showed that 472 genes were

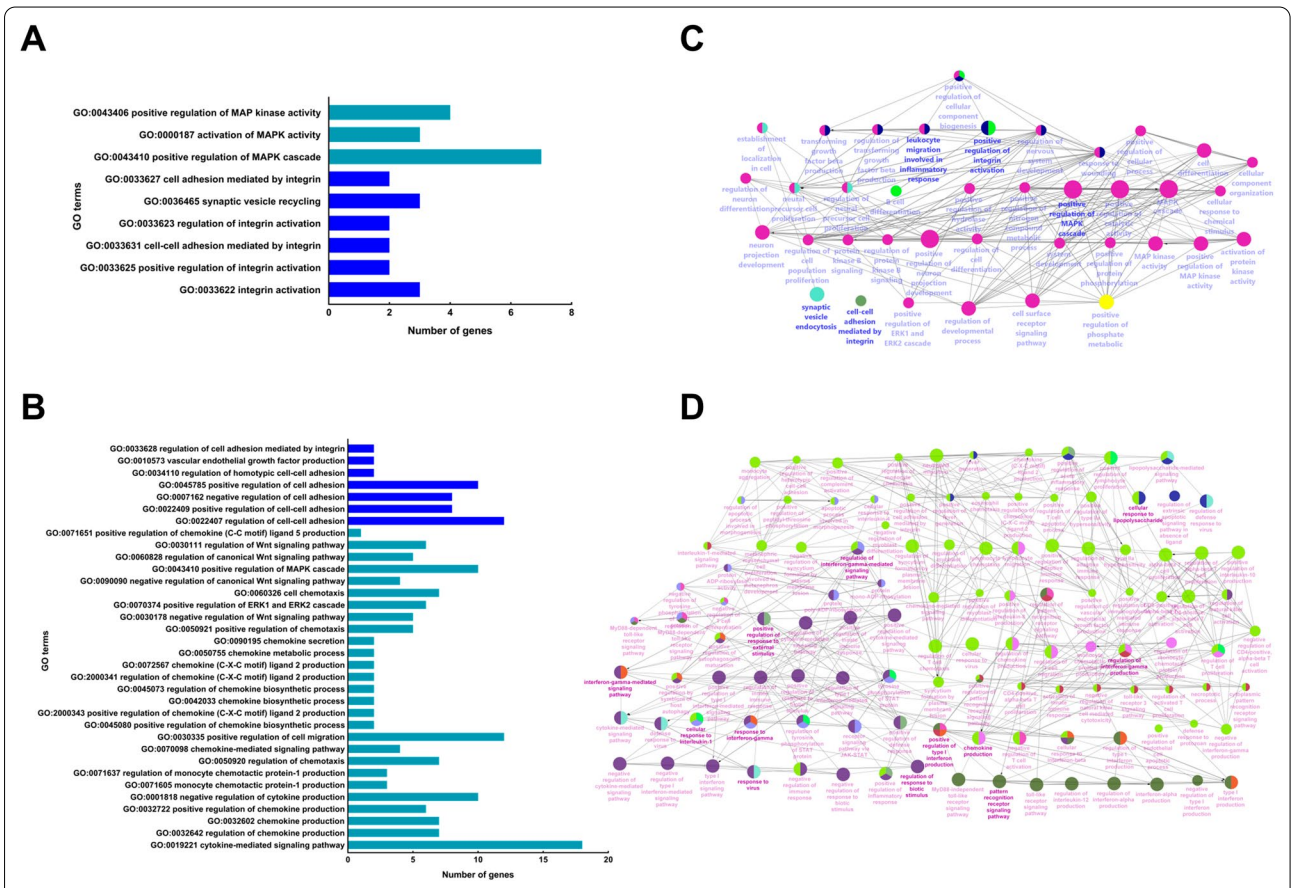

Fig. 1 Gene ontology (GO) term analysis. **A** GO term analysis of upregulated genes between peroxiredoxin (Prx) II$^{+/+}$ and Prx II$^{-/-}$ dermal mesenchymal stem cells (DMSCs) derived from mice. **B** GO term analysis of the downregulated genes between Prx II$^{+/+}$ and Prx II$^{-/-}$ DMSCs derived from mice. The horizontal axis represents the gene numbers. The vertical axis represents enriched GO terms. We divided differential GO terms into cell migration (dark blue) and cell-to-cell adhesion (light blue) to facilitate differentiation. **C**, **D** ClueGo was used to analyze the interaction networks in enriched biological processes. Multi-colored dots indicate the involvement of multiple biological processes

Table 2 GO terms associated with cell migration

GO ID	GO Term	Genes
GO:0030335	Positive regulation of cell migration	Lgals9/Col18a1/Bmp7/Cd274/Gli1/Il1b /Cxcl9/Gpnmb/Ret/Pycard/Cxcl10/Ccl5
GO:0032642	Regulation of chemokine production	Lgals9/Mcoln2/Apod/Il1b/Pycard /Tlr3/Ccl5
GO:0032602	Chemokine production	Lgals9/Mcoln2/Apod/Il1b/Pycard /Tlr3/Ccl5
GO:0032722	Positive regulation of chemokine production	Lgals9/Mcoln2/Il1b/Pycard/Tlr3/Ccl5
GO:0001818	Negative regulation of cytokineproduction	Lgals9/Cd274/Dhx58/Apod/Nmi/Gpnmb /Pycard/Trim30a/Pml/Tigit
GO:0071605	Monocyte chemotactic protein-1 production	Mcoln2/Apod/Il1b
GO:0071637	Regulation of monocyte chemotactic protein-1 production	Mcoln2/Apod/Il1b
GO:0050920	Regulation of chemotaxis	Il16/Slit1/Il1b/Cxcl9/Cxcl10/Ccl5/Agrn
GO:0070098	Chemokine-mediated signaling pathway	Ccl8/Cxcl9/Cxcl10/Ccl5
GO:0019221	Cytokine-mediated signaling pathway	Ccl8/Irf1/Parp9/Irf7/Stat1/Nmi/Il1b/Zbp1 /Adar/Cxcl9/Pycard/Parp14/Cxcl10/Ccl5 /Stat2/Irgm1/Irgm2/Nlrc5
GO:0045080	Positive regulation of chemokine biosynthetic process	Il1b/Tlr3
GO:2000343	Positive regulation of chemokine (C-X-C motif) ligand 2 production	Mcoln2/Ccl5
GO:0042033	Chemokine biosynthetic process	Il1b/Tlr3
GO:0045073	Regulation of chemokine biosynthetic process	Il1b/Tlr3
GO:2000341	Regulation of chemokine (C-X-C motif) ligand 2 production	Mcoln2/Ccl5
GO:0072567	Chemokine (C-X-C motif) ligand 2 production	Mcoln2/Ccl5
GO:0050755	Chemokine metabolic process	Il1b/Tlr3
GO:0090195	Chemokine secretion	Mcoln2/Pycard
GO:0050921	Positive regulation of chemotaxis	Il16/Il1b/Cxcl9/Cxcl10/Ccl5
GO:0030178	Negative regulation of Wnt signaling pathway	Gli1/Ddit3/Draxin/Rnf213/Lats2
GO:0070374	Positive regulation of ERK1 and ERK2 cascade	Ccl8/C3/Il1b/Gpnmb/Pycard/Ccl5
GO:0060326	Cell chemotaxis	Il16/Ccl8/Il1b/Arhgef16/Cxcl9/Cxcl10/Ccl5
GO:0090090	Negative regulation of canonical Wnt signaling pathway	Gli1/Ddit3/Draxin/Lats2
GO:0043410	Positive regulation of MAPK cascade	Prdx2/Ccl8/C1qtnf1/Cd40/C3/Il1b /Gpnmb/Pycard/Tlr3/Ccl5
GO:0060828	Regulation of canonical Wnt signaling pathway	Gli1/Ddit3/Draxin/Rspo2/Lats2
GO:0030111	Regulation of Wnt signaling pathway	Gli1/Ddit3/Draxin/Rspo2/Rnf213/Lats2
GO:0071651	Positive regulation of chemokine (C–C motif) ligand 5 production	Mcoln2
GO:0043410	Positive regulation of MAPK cascade	Ngfr/Cx3cl1/Npnt/Cd24a/Alk/Ntrk3/Ighm
GO:0000187	Activation of MAPK activity	Alk/Ntrk3/Ighm
GO:0043406	Positive regulation of MAP kinase activity	Cd24a/Alk/Ntrk3/Ighm

differentially expressed (176 upregulated and 296 downregulated) [29]. We used the DAVID software for GO term enrichment analysis of the DEGs, using a threshold of $P<0.05$. The results showed that the upregulated genes were significantly enriched in the biological process terms positive regulation of the MAPK cascade (GO:0043410) and cell adhesion mediated by integrin (GO:0033631) (Fig. 1A). Downregulated genes were significantly enriched in the biological process terms positive regulation of cell migration (GO:0030335) and regulation of cell adhesion (GO:0022407) (Fig. 1B). Interestingly, these DEG-enriched GO terms were mainly related to cell migration and intercellular adhesion. We used the Cytoscape plug-in ClueGo to visualize the interaction network of biological processes, as shown in Fig. 1C, D. Each node represents a GO term, and nodes of the same color represent shared or similar genes among them. Therefore, nodes of the same color represent shared or similar genes, and different colors indicate that they are enriched with different genes. These results indicated that Prx II is involved in regulating DMSC homing.

Table 3 GO terms associated with cell–cell adhesion

GO ID	GO term	Genes
GO:0022407	Regulation of cell–cell adhesion	Lgals9/Prdx2/Bmp7/Cd274/C1qtnf1/Irf1/Il1b/Gpnmb/Pycard/Ccl5/H2-T23/Tigit
GO:0022409	Positive regulation of cell–cell adhesion	Lgals9/Bmp7/Cd274/Irf1/Il1b/Pycard/Ccl5/H2-T23
GO:0007162	Negative regulation of cell adhesion	Lgals9/Prdx2/Cd274/C1qtnf1/Irf1/Apod/Gpnmb/Tigit
GO:0045785	Positive regulation of cell adhesion	Lgals9/Bmp7/Cd274/Irf1/Smoc2/Il1b/Ret/Pycard/Ccl5/H2-T23
GO:0034110	Regulation of homotypic cell–cell adhesion	C1qtnf1/Ccl5
GO:0010573	Vascular endothelial growth factor production	C3/Il1b
GO:0033628	Regulation of cell adhesion mediated byintegrin	Ret/Ccl5
GO:0033622	Integrin activation	Cdh17/Cx3cl1/Cd24a
GO:0033625	Positive regulation of integrin activation	Cdh17/Cd24a
GO:0033631	Cell–cell adhesion mediated by integrin	Npnt/Cd24a
GO:0033623	Regulation of integrin activation	Cdh17/Cd24a
GO:0036465	Synaptic vesicle recycling	Amph/Syt1/Cd24a
GO:0033627	Cell adhesion mediated by integrin	Npnt/Cd24a

PPI network analysis of cell migration and intercellular adhesion

To investigate the molecular mechanism underlying Prx II-regulated DMSC homing, we screened GO terms (Tables 2, 3) related to cell migration and intercellular adhesion, as they are closely associated with stem cell homing. The cell migration and cell adhesion genes were separately used to construct PPI networks using the STRING database. The networks were visualized and analyzed using Cytoscape. Analysis of the nodal properties in each network revealed an average degree of 10.372 for cell migration nodes and of 2.6154 for intercellular adhesion nodes. Degree refers to how many nodes this node is connected to. The more connected nodes, the more this gene is in a central position of the regulatory network (i.e., a hub gene). Here, we calculated the average degree of DEGs in cell migration and cell adhesion, which were 10.372 and 2.6154, respectively. We then considered higher than average degree for DEGs as a condition for hub gene screening. Three genes were identified as hub genes for cell migration: Cd274 antigen (*Cd274*), interleukin 1 beta (*Il1B*), and signal transducer and activator of transcription 1 (*Stat1*). Three genes were identified as hub genes for intercellular adhesion: *Cd274*, *Il1B*, and *Ccl5* (Fig. 2A, B and Table 4). Next, we detected the mRNA expression levels of *Cd274*, *Il1b*, *Stat1*, and *Ccl5* in the two cell types using RT-qPCR, and the results were consistent with the RNA sequencing results (Fig. 2C). The expression of Prx II in the NC and WT cells was determined using immunoblotting. Prx II protein was successfully expressed in the WT group (Fig. 2D). When Prx II was expressed in Prx II$^{-/-}$ DMSCs cells, the expression levels of *Cd274*, *Il1b*, *Stat1*, and *Ccl5* in WT cells were significantly higher than those in NC cells (Fig. 2E). Together, these results suggested that Prx II regulates DMSC homing by regulating these hub genes.

Further miRNA mining and interaction network analysis

As miRNAs recognize their target mRNAs through base complementary pairing, we predicted that Prx II regulates mRNAs via miRNAs and therefore explored how Prx II regulates hub genes. Four genes related to DMSC homing were screened, and gene-miRNA analysis was performed using miRWalk. The intersection of the miRNAs predicted by the TargetScan, miRanda, miRDB, miRWalk, and RNA22 databases was selected as the prediction result. The selection threshold was set to $P<0.05$. The minimum sequence length was a 7-mer, and the target gene-binding region was the 3′ untranslated region. Cytoscape was used to draw the interaction network, as shown in Fig. 3A. We selected miRNAs with gene cross-linking (> 2) for further study (Fig. 3A and Table 5). Three miRNAs were predicted, and RT-qPCR was used to verify their expression levels in Prx II$^{+/+}$and Prx II$^{-/-}$ DMSCs. Only miR-351 was found to be altered (Fig. 3B). After Prx II rescue in Prx II$^{-/-}$ DMSCs, the miR-351 expression levels in WT cells were significantly higher than those in NC cells (Fig. 3C). These findings indicated that Prx II may regulate Il1b/Stat1 through miR-351 to regulate stem cell homing.

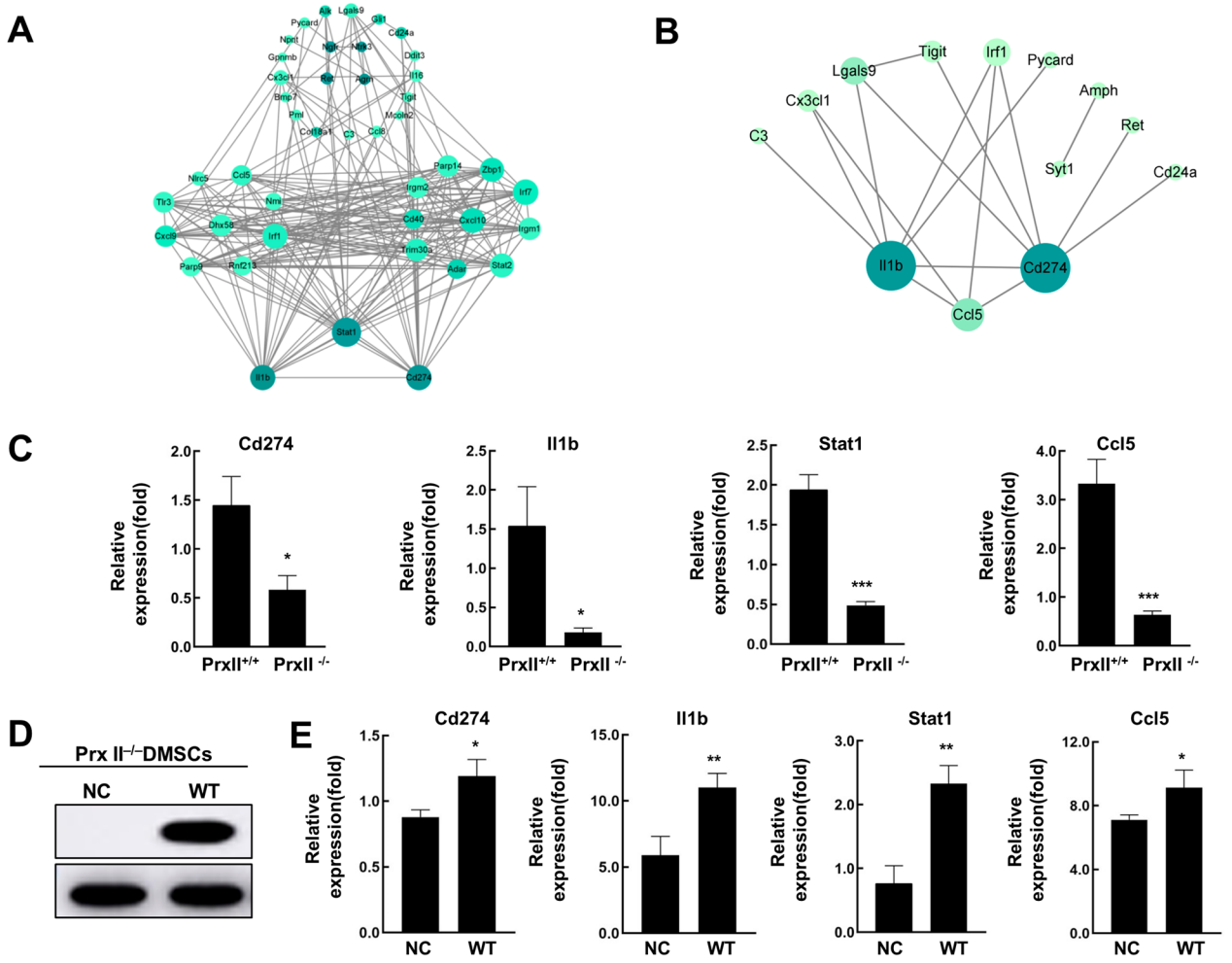

Fig. 2 Protein–protein interaction (PPI) networks of cell migration and intercellular adhesion biological processes. **A**, **B** PPI network constructed to screen hub genes. Node color: shades of green to blue represent high to low values of betweenness centrality (BC). Node size: circle size represents the node degrees. Larger and darker-colored nodes represent genes with more links. **C**, **D** Expression levels of hub genes detected using RT-qPCR. Data are presented as the mean ± SD from at least three independent experiments (*$P < 0.05$, **$P < 0.01$, ***$P < 0.001$)

LncRNA prediction

To explore the specific underlying molecular mechanism, we searched for molecules upstream of miRNAs.

Table 4 Key genes selected based on visualize parameters like BC and degree

Network name	Gene	Degree	BC	AD
Cell migration	Cd274	21	0.1879	10.372
	Il1b	21	0.1185	
	Stat1	6	0.2435	
Cell–cell adhesion	Il1b	7	0.4815	2.6154
	Cd274	7	0.0519	
	Ccl5	4	0.4926	

BC betweenness centrality, *AD* average degree of all nodes

We evaluated lncRNAs, and the lncRNA of muu-miR-351 was predicted using Starbase. Cytoscape was used to draw the interaction networkshown in Fig. 4A. Next, we analyzed differentially expressed lncRNAs between Prx $II^{+/+}$ and Prx $II^{-/-}$ DMSCs using lncRNA sequencing. We identified 464 differentially expressed lncRNAs (262 upregulated and 202 downregulated). The differentially expressed lncRNAs were plotted in a heat map (Fig. 4B). Interestingly, only lncRNA Tctn2 was significantly different ($P < 0.001$) (Table 6). The results showed that after Prx II knockout, Tctn2 expression decreased, which was consistent with the sequencing results (Fig. 4C). Similarly, Tctn2 expression was measured in NC and WT cells; it was increased in WT cells when compared with NC cells (Fig. 4D).

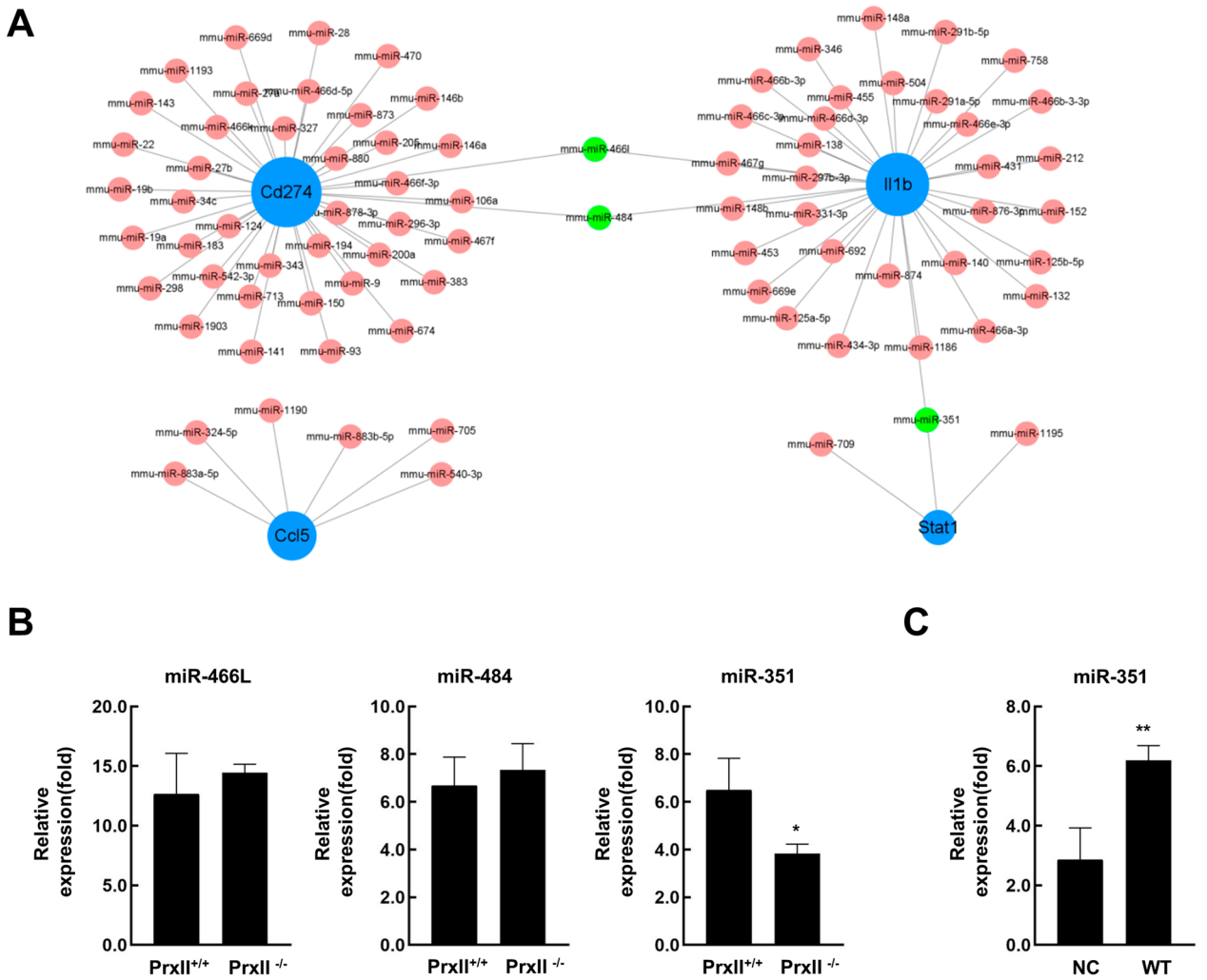

Fig. 3 Interaction network of hub genes and their target miRNAs. **A** Network of genes and miRNAs. **B**, **C** Genes are colored in blue, and the node size represents the number of targeted miRNAs. miRNAs are colored in red; miRNAs targeting more than two genes are colored in green. The expression levels of miRNAs targeting more than two hub genes were detected using RT-qPCR. Data are presented as the mean ± SD from at least three independent experiments (*$P < 0.05$, **$P < 0.01$, ***$P < 0.001$)

Discussion

During tissue injury, various chemokines, adhesion factors, and growth factors are locally produced and secreted, thus initiating MSC homing [30, 31]. The interactions between chemical factors and their receptors in the internal environment guide stem cells to the lesion site [30, 31]. Several studies have shown that MSC homing involves substances very similar to those involved in white blood cell homing to inflamed tissues [32]. MSCs show strong adhesion, crawling, diffusion, and transendothelial cell migration in the treatment of various diseases [32]. Furthermore, the homing rate of MSCs directly determines their therapeutic effect. Therefore, identifying methods to enhance or mediate the migration ability of stem cells is a promising approach for improving the recruitment of stem cells to benefit patients.

The migration and recruitment of MSCs to the target site is essential for the success of MSC-based therapies [32]. In this study, we investigated Prx $II^{+/+}$ and Prx $II^{-/-}$ DMSCs by RNA sequencing analysis. We found that the

Table 5 miRNAs and its target genes

miRNA	Genes targeted By miRNA	Gene count
mmu-miR-466l	Cd274,Il1b	2
mmu-miR-484	Cd274,Il1b	2
mmu-miR-351	Stat1,Il1b	2

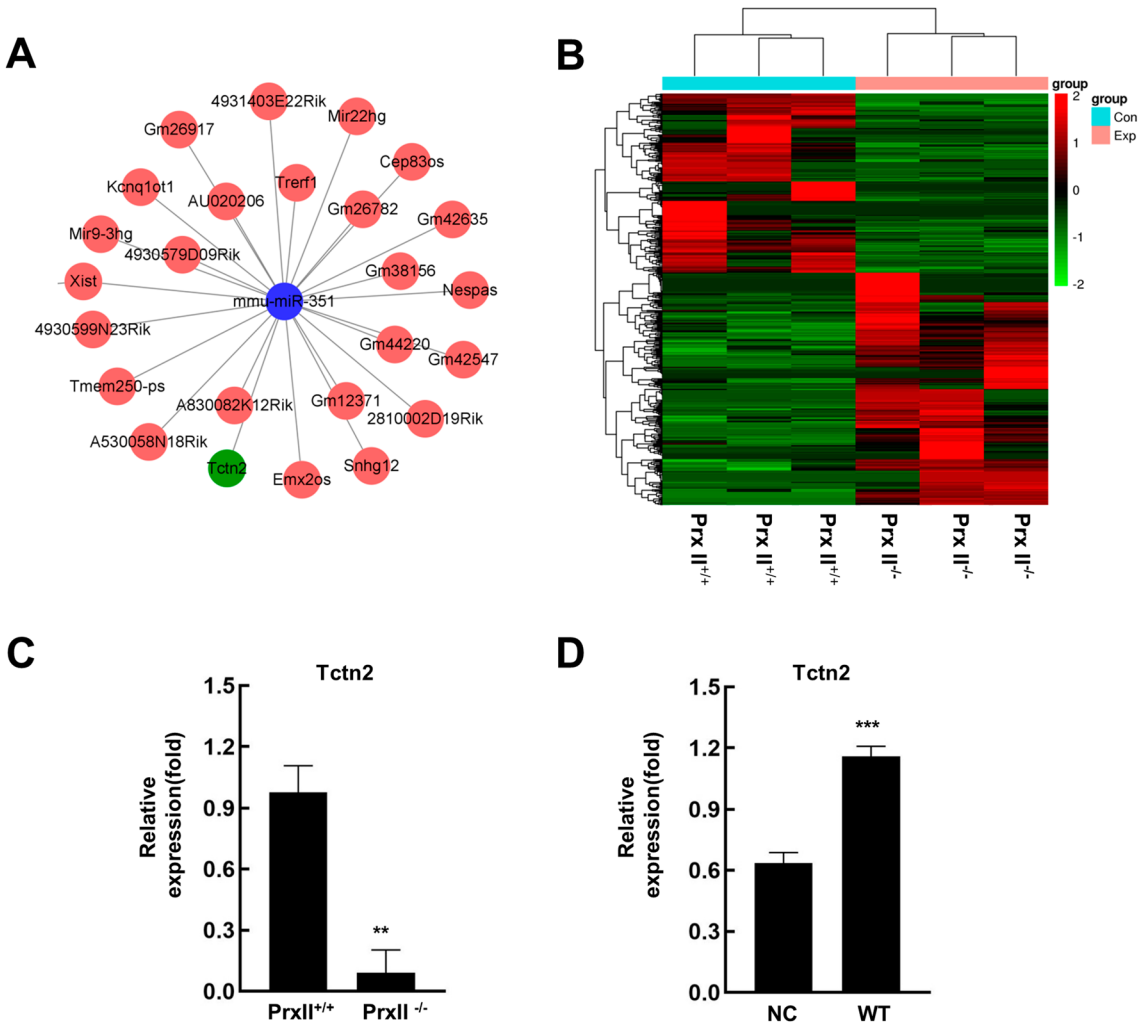

Fig. 4 Interaction network between micro-RNAs (miRNAs) and long non-coding RNAs (lncRNAs). **A** lncRNAs–miRNA network. miRNAs are colored in blue, lncRNAs are colored in red, and differentially expressed lncRNAs are colored in green. **B** Heat map of the differentially expressed lncRNAs of three Prx $II^{+/+}$ dermal mesenchymal stem cells (DMSCs) and peroxiredoxin (Prx) $II^{-/-}$ DMSCs. Each row represents a differential lncRNA, lncRNAs shown in red are upregulated and those shown in green are downregulated. **C** Expression levels of the lncRNA Tctn 2 in Prx $II^{+/+}$ DMSCs and Prx $II^{-/-}$ DMSCs as determined by RT-qPCR. **D** Expression levels of Tctn 2 in NC and WT cells by RT-qPCR. Data are presented as the mean ± SD from at least three independent experiments (*$P < 0.05$, **$P < 0.01$, ***$P < 0.001$)

DEGs were mainly enriched in cell migration and intercellular adhesion. In a PPI network, *Cd274*, *Il1b*, *Stat1*, and *Ccl5* were identified as hub genes. Studies have shown that NKX2-1-AS1 transcripts control cell adhesion and migration of lung tumor cell lines by regulating CD274 [33]. Oviduct epithelial cell culture medium supplemented with IL1B significantly induced polymorph nuclear neutrophil migration [34]. The CCL5/CCR5 axis has been shown to enhance tumor local invasiveness by inducing intracellular calcium-dependent signaling cascades and matrix metalloproteinase [35]. The transcription factor STAT1 promotes the migration of nasopharyngeal carcinoma cells [36]. In addition, STAT1 regulates CD274 to participate in pancreatic cancer progression [37]. We found that the expression level of miR-351 decreased after Prx II knockout, and miR-351 was predicted to regulate the expression of Stat1, indicating a positive regulatory relationship between miR-351 and Stat1. Through further analysis of the underlying mechanism, we identified an lncRNA upstream of miR-351 (Tctn2) and found that Prx II is involved in the regulation of this lncRNA. In summary, these data indicate that Prx II regulates the homing of DMSCs by regulating the Tctn2/mir-351/Stat1/Il1b axis (Fig. 5). The study findings provide a new approach for treating various diseases using stem cells.

Table 6 List of differentially expressed LncRNAs

Transcript ID	lncRNA Name	FPKM Prx II$^{+/+}$ (Avg)	FPKM Prx II$^{-/-}$ (Avg)	P value
ENSMUST00000130912.2	Tctn2	1.653501667	0	5.2906E−10
ENSMUST00000194601.1	Gm38156	0	0	NA
ENSMUST00000133808.1	Tmem250-ps	33.22795067	33.29932067	0.91251898
ENSMUST00000152313.1	2810002D19Rik	0.996595333	1.222854333	0.414528527
ENSMUST00000128469.7	A530058N18Rik	0	0	NA
ENSMUST00000143738.1	Nespas	0.593392667	0.190762667	0.085510904
ENSMUST00000144029.1	Gm12371	0	0.129042	0.091113808
ENSMUST00000144705.7	Snhg12	0.718972333	0.932234333	0.72991711
ENSMUST00000200266.1	Gm42635	0.042979	0.164026333	0.189922154
ENSMUST00000201159.1	Gm42547	0.653974667	0.911198333	0.447234079
ENSMUST00000146981.1	4930599N23Rik	0.896182333	0.506518333	0.310292806
ENSMUST00000203784.1	Gm44220	0.101183333	0.096917667	0.986736134
ENSMUST00000132321.1	4930579D09Rik	0	0	NA
ENSMUST00000181224.1	AU020206	4.009352333	3.946091667	0.99363201
ENSMUST00000181511.8	Mir9-3hg	0	0.001095333	0.847176253
ENSMUST00000185789.1	Kcnq1ot1	0.004885	0.008278333	0.622600707
ENSMUST00000181906.2	Cep83os	0.047183	0.036257333	0.868651086
ENSMUST00000134345.1	Mir22hg	0.795591	0.876390333	0.806646032
ENSMUST00000134705.1	A830082K12Rik	0.158965	0.386743667	0.372800291
ENSMUST00000181482.1	Gm26782	0.153841	0.140497	0.955462085
ENSMUST00000182520.1	Gm26917	1.266974	1.744698667	0.449954947
ENSMUST00000077951.13	Trerf1	0	0	NA
ENSMUST00000177048.1	4931403E22Rik	0	0.010921	0.722756137
ENSMUST00000136990.2	Emx2os	0.554004333	0.508853	0.88919062
ENSMUST00000153883.2	Xist	0.250889	0.415639	0.528732566

Prx II, as a peroxidase, plays an important role in maintaining the concentration of hydrogen peroxide [38]. When the TNF-α receptor is activated, Prx I and Prx II modulate the intracellular hydrogen peroxide level, thus regulating cell signal transduction [39]. Prx II not only acts as a peroxide reductase, but also regulates signal transduction by regulating the redox state of protein kinase [40]. We previously found that Prx II can regulate the senescence of DMSCs and determined the regulatory mechanism in detail, providing a foundation for analysis of the relationship between Prx II and the regulation of stem cell function [19, 20]. In this study, Prx II was identified as an important regulator of stem cell homing. Although numerous studies have investigated the use of stem cells in the treatment of various diseases, including cancers, no clinically significant treatment results have been obtained, likely because stem cells have different proliferation mechanisms in the body. As this study was based on in vitro and in silico analyses, the clinical relevance of the findings requires further study.

We identified 464 differentially expressed lncRNAs after knocking down Prx II, suggesting that Prx II is a key target for lncRNA regulation. Studies have shown that lncRNAs have many mechanisms of action. LncRNAs (1) induce transcription in the upstream promoter region of the protein-coding gene, thus interfering with the expression of adjacent protein-coding genes, (2) inhibit RNA polymerase II or mediate chromatin remodeling and histone modification, thus affecting gene expression, and (3) bind to specific proteins to regulate their activity [41]. Thus, there may be a mutual regulatory relationship between genes and lncRNAs. Elucidating the specific regulatory mechanism of Prx II and lncRNAs in stem cell homing will be the focus of our further research.

In conclusion, using RNA sequencing and bioinformatics analyses, we found that DEGs were mainly enriched in the GO terms cell migration and intercellular adhesion after Prx II knockout, and that Prx II regulates the homing of DMSCs by regulating the lncRNA Tctn2/mir-351/Stat1/Il1b axis. It is of great significance

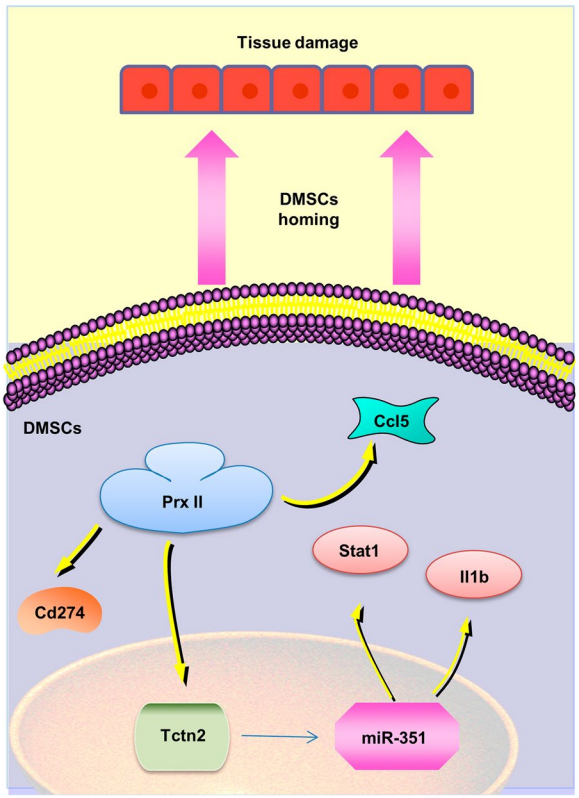

Fig. 5 Peroxiredoxin (Prx) II regulates dermal mesenchymal stem cell (DMSC) homing. Prx II participates in DMSC homing by downregulating the expression of hub genes, including *Cd274*, *Il1b*, *Stat1*, and *Ccl5*, related to stem cell migration and adhesion. Further, Prx II regulates the Tctn2/miR-351/Stat1/Ccl5 axis involved in DMSC homing so as to repair damaged tissues

to clarify the specific molecular mechanism of stem cell homing and external regulation of the target to improve the homing efficiency of MSCs.

Abbreviations

CCL5: Chemokine (C–C motif) ligand 5; DEGs: Differentially expressed genes; DMSCs: Dermal mesenchymal stem cells; GO: Gene Ontology; MSCs: Mesenchymal stem cells; Prx: Peroxiredoxin; PPI: Protein–protein interaction network; VLA-4: Vascular cell adhesion molecule-1/very late antigen-4.

Acknowledgments

This research was supported by a postgraduate project grant to innovate scientific research (YJSCX2021-Y102) from Heilongjiang Bayi Agricultural University, and by the Natural Science Foundation of Heilongjiang Province of China (LH2021C061).

Author contributions

YHH, YYM, and TK contributed to the conception of the study, writing of the manuscript, and performing the literature search. YYF and HYX performed data analysis. YHH, MHJ, and HNS performed analysis and assessed the quality of the study. YHH, YYM, and TK confirm the authenticity of all the raw. YHH and TK conceived and designed the project. All authors read and approved the final manuscript.

Funding

This research was supported by the Basic Science Research Program of the National Research Foundation of Korea (NRF) funded by the Ministry of Education (2020R1I1A2052417), KRIBB-RBM0112213.

Availability of data and materials

The datasets used and analyzed in this study are available from the corresponding author upon reasonable request.

Declarations

Competing interests

The authors declare that they have no competing interests.

Received: 22 February 2022 Accepted: 23 May 2022
Published online: 15 June 2022

References

1. Naji A, Eitoku M, Favier B, Deschaseaux F, Rouas-Freiss N, Suganuma N (2019) Biological functions of mesenchymal stem cells and clinical implications. Cell Mol Life Sci 76:3323–3348
2. De Becker A, Van Riet I (2016) Homing and migration of mesenchymal stromal cells: how to improve the efficacy of cell therapy? World J Stem Cells 03:20–34
3. Katrin Z, Dominika L, Rayyan H, Alfred G, Johannes W, Ljubica M, Denise T, Andreas S, Susanne W, Gerald Z (2018) Matrix metalloproteinase-2 impairs homing of intracoronary delivered mesenchymal stem cells in a porcine reperfused myocardial infarction: comparison with intramyocardial cell delivery. Front Bioeng Biotechnol 6:35
4. Song Y (2012) Immunomodulatory properties of mesenchymal stem cells and their therapeutic applications. Arch Pharmacal Res 35:213–221
5. Galipeau J (2013) The mesenchymal stromal cells dilemma–does a negative phase III trial of random donor mesenchymal stromal cells in steroid-resistant graft-versus-host disease represent a death knell or a bump in the road? Cytotherapy 15:2–8
6. Smith H, Whittall C, Weksler B, Middleton J (2012) Chemokines stimulate bidirectional migration of human mesenchymal stem cells across bone marrow endothelial cells. Stem Cells Dev 21:476–486
7. Asfour I, Afify H, Elkourashy S, Ayoub M, Kamal G, Gamal M, Elgohary G (2017) CXCR4 (CD184) expression on stem cell harvest and CD34+ cells post-transplant. Hematol/Oncol Stem Cell Ther 10:63–69
8. Kroeze KL, Jurgens WJ, Doulabi BZ, Van Milligen FJ, Scheper RJ, Gibbs S (2009) Chemokine-mediated migration of skin-derived stem cells: predominant role for CCL5/RANTES. J Invest Dermatol 129:1569–1581
9. Lee JK, Schuchman EH, Jin HK, Bae JS (2012) Soluble CCL5 derived from bone marrow-derived mesenchymal stem cells and activated by amyloid β ameliorates Alzheimer's Disease in Mice by recruiting bone marrow-induced microglia immune responses. Stem Cells 30:1544–1555
10. Jie Z, Zhou Z, Yong L, Jian Z (2009) Fractalkine and CX3CR1 are involved in the migration of intravenously grafted human bone marrow stromal cells toward ischemic brain lesion in rats. Brain Res 1287:173–183
11. Clements LE, Garvican ER, Dudhia J, Smith RKW (2016) Modulation of mesenchymal stem cell genotype and phenotype by extracellular matrix proteins. Connect Tissue Res 57:443–453
12. Rüster B, Göttig S, Ludwig RJ, Bistrian R, Henschler R (2006) Mesenchymal stem cells display coordinated rolling and adhesion behavior on endothelial cells. Blood 108:3938–3944
13. Sang WK, Rhee SG, Chang TS, Jeong W, Min HC (2005) 2-Cys peroxiredoxin function in intracellular signal transduction: therapeutic implications. Trends Mol Med 11:571–578
14. Rong W, Wei J, Zhang S, Wu X, Fu Z (2016) Peroxiredoxin 2 is essential for maintaining cancer stem cell-like phenotype through activation of Hedgehog signaling pathway in colon cancer. Oncotarget 7:86816–86828

15. Kim SU, Park YH, Kim JM, Sun HN, Song IS, Huang SM, Lee SH, Chae JI, Hong S, Sik Choi S, Choi SC (2014) Dominant role of peroxiredoxin/JNK axis in stemness regulation during neurogenesis from embryonic stem cells. Stem Cells 32:998–1011
16. Kwon T, Bak Y, Park Y, Jang G, Nam J, Yoo JE, Park YN, Bak IS, Kim J, Yoon D (2016) Peroxiredoxin II is essential for maintaining stemness by redox regulation in liver cancer cells. Stem Cells 34:1188–1197
17. Nisansala C, Dong J, Taeho K (2018) Peroxiredoxin II regulates cancer stem cells and stemness-associated properties of cancers. Cancers 10:305
18. Han YH, Jin MH, Jin YH, Nan-Nan YU, Liu J, Zhang YQ, Cui YD, Wang AG, Lee DS, Kim SU (2020) Deletion of peroxiredoxin II inhibits the growth of mouse primary mesenchymal stem cells through induction of the G0/G1 cell-cycle arrest and activation of AKT/GSK3β/β-catenin signaling. In Vivo 34:133–141
19. Han Y-H, Mao Y-Y, Yu N-N, Jin M-H, Jin Y-H, Wang A-G, Zhang Y-Q, Shen G-N, Cui Y-D, Yu L-Y, Lee D-S, Jo Y-J, Sun H-N, Kwon J, Kwon T (2020) RNA sequencing reveals that Prx II gene knockout can down-regulate the allograft rejection of dermal mesenchymal stem cells. Appl Biol Chem 63:30
20. Jin MH, Yu NN, Jin YH, Mao YY, Feng L, Liu Y, Wang AG, Sun HN, Kwon T, Han YH (2021) Peroxiredoxin II with dermal mesenchymal stem cells accelerates wound healing. Aging (Albany NY) 13:13926–13940
21. Zong Z, Nan L, Ran X, Su Y, Shen Y, Shi CM, Cheng TM (2011) Isolation and characterization of two kinds of stem cells from the same human skin back sample with therapeutic potential in spinal cord injury. PLoS ONE 7:e50222
22. Han YH, Jin MH, Jin YH, Nan-Nan YU, Liu J, Zhang YQ, Cui YD, Wang AG, Lee DS, Kim SU (2020) Deletion of peroxiredoxin II inhibits the growth of mouse primary mesenchymal stem cells through induction of the G 0/G 1 cell-cycle arrest and activation of AKT/GSK3β/β-catenin signaling. In Vivo (Athens, Greece) 34:133–141
23. Zong Z, Li N, Ran X, Su Y, Shen Y, Shi CM, Cheng TM (2012) Isolation and characterization of two kinds of stem cells from the same human skin back sample with therapeutic potential in spinal cord injury. PLoS ONE 7:e50222
24. Sherman BT, Da WH, Tan Q, Guo Y, Bour S, Liu D, Stephens R, Baseler MW, Lane CH, Lempicki RA (2007) DAVID Knowledgebase: a gene-centered database integrating heterogeneous gene annotation resources to facilitate high-throughput gene functional analysis. BMC Bioinform 8:426
25. Shannon P (2003) Cytoscape: a software environment for integrated models of biomolecular interaction networks. Genome Res 13:2498–2504
26. Damian S, Morris JH, Helen C, Michael K, Stefan W, Milan S, Alberto S, Doncheva NT, Alexander R, Peer B (2017) The STRING database in 2017: quality-controlled protein–protein association networks, made broadly accessible. Nucleic Acids Res 45:D362–D368
27. Dweep H, Sticht C, Pandey P, Gretz N (2011) MiRWalk—Database: prediction of possible miRNA binding sites by "walking" the genes of three genomes. J Biomed Inform 44:839–847
28. Li JH, Liu S, Hui Z, Qu LH, Yang JH (2014) starBase v2.0: decoding miRNA-ceRNA, miRNA-ncRNA and protein–RNA interaction networks from large-scale CLIP-Seq data. Nucleic Acids Res 42:D92–D97
29. Han YH, Mao YY, Yu N, Jin MH, Kwon T (2020) RNA sequencing reveals that Prx II gene knockout can down-regulate the allograft rejection of dermal mesenchymal stem cells. Appl Biol Chem 63:1–10
30. Renata, and Szydlak, (2019) Mesenchymal stem cells' homing and cardiac tissue repair. Acta Biochim Pol 66:483–489
31. Kang SK, Shin IS, Ko MS, Jo JY, Ra JC (2012) Journey of mesenchymal stem cells for homing: strategies to enhance efficacy and safety of stem cell therapy. Stem Cells Int 2012:342968
32. De Becker A, Riet IV (2016) Homing and migration of mesenchymal stromal cells: how to improve the efficacy of cell therapy? World J Stem Cells 8:73–87
33. Kathuria H, Millien G, McNally L, Gower AC, Tagne J-B, Cao Y, Ramirez MI (2018) NKX2-1-AS1 negatively regulates CD274/PD-L1, cell-cell interaction genes, and limits human lung carcinoma cell migration. Sci Rep 8:14418
34. Nakamura Y, Aihara R, Iwata H, Kuwayama T, Shirasuna K (2021) IL1B triggers inflammatory cytokine production in bovine oviduct epithelial cells and induces neutrophil accumulation via CCL2. Am J Reprod Immunol 85:e13365
35. Yu-Ju Wu C, Chen C-H, Lin C-Y, Feng L-Y, Lin Y-C, Wei K-C, Huang C-Y, Fang J-Y, Chen P-Y (2020) CCL5 of glioma-associated microglia/macrophages regulates glioma migration and invasion via calcium-dependent matrix metalloproteinase 2. Neuro Oncol 22:253–266
36. Ai J, Tan G, Wang T, Li W, Gao R, Song Y, Xiong S, Qing X (2021) Transcription factor STAT1 promotes the proliferation, migration and invasion of nasopharyngeal carcinoma cells by upregulating. Future Oncol 17:57–69
37. Zhang H, Zhu C, He Z, Chen S, Li L, Sun C (2020) LncRNA PSMB8-AS1 contributes to pancreatic cancer progression via modulating miR-382-3p/STAT1/PD-L1 axis. J Exp Clin Cancer Res 39:179
38. Rhee SG, Woo HA, Kil IS, Bae SH (2012) Peroxiredoxin functions as a peroxidase and a regulator and sensor of local peroxides. J Biol Chem 287:4403–4410
39. Kang SW, Chae HZ, Seo MS, Kim K, Baines IC, Rhee SG (1998) Mammalian peroxiredoxin isoforms can reduce hydrogen peroxide generated in response to growth factors and tumor necrosis factor-α. J Biol Chem 273:6297–6302
40. Sobotta MC, Liou W, Stcker S, Talwar D, Dick TP (2014) Peroxiredoxin-2 and STAT3 form a redox relay for H2O2 signaling. Nat Chem Biol 11:64–70
41. Rinn JL, Kertesz M, Wang JK, Squazzo SL, Xu X, Brugmann SA, Goodnough LH, Helms JA, Farnham PJ, Segal E, Chang HY (2007) Functional demarcation of active and silent chromatin domains in human HOX loci by noncoding RNAs. Cell 129:1311–1323

Publisher's Note